ISSN 1392 - 1207. MECHANIKA. 2010. Nr.1(81)

The effect of lubricant rheology on piston skirt/cylinder contact for an internal combustion engine

A. Kellaci*, R. Mazouzi, B. Khelidj***, A. Bounif******
**Khemis miliana University, Thenia road, Ain Defla, Algeria, E-mail: akellaci@yahoo.fr*
***Solides Mécanique laboratory, University of Poitiers, France, E-mail: mazouzi_r@yahoo.fr*
****Khemis miliana University, Thenia road, Ain Defla, Algeria, E-mail: bkhelidj@orange.fr*
*****University of Science and Technology, Oran, Algeria, E-mail: bounif@univ-usto.dz*

1. Introduction

One method utilized to promote energy savings in internal combustion engines is to reduce the power loss caused by mechanical friction on lubricated surfaces of engines. Most of the mechanical friction power loss in the internal combustion engines occurs at the contact liner/piston rings and liner/skirt. Factors that affect piston skirt lubrication characteristics are the piston design parameters (radial clearance, roughness, skirt profile, etc.), the viscosity of oil as well as the operating conditions (rotational speed, gas pressure, etc.).

The variation of lubricant viscosity with temperature is crucial insofar as it affects engine's performance. Unfortunately, these effects are typically ignored in the models that are used to design engine components. Here the viscosity of the oil film is generally assumed to be constant over the cycle [1-3]. Richardson [4] carried out a theoretical investigation into the effects of viscosity variation and the effect of temperature gradient on lubrication. He concluded that temperature of the oil film is equivalent to the temperature of cylinder surface with the experimental results corresponding to the theoretical results. On this basis, other researchers have made tests with variable viscosity depending on the skirt surface temperature. Taylor [5] studied the sensitivity of diesel engine friction with the lubricant viscosity varying according to shear rate and temperature. His work helped to determine the proportions of hydrodynamic friction and boundary friction in the engine.

This study examines the effects of lubricant viscosity and its variation during the engine cycle on the tribological characteristics of piston skirt/liner contact and friction as the oil film thickness, hydrodynamic pressure and the friction force. The model takes into account the waviness of surface. A brief study of the boundary friction coefficient is also included as this can have a large effect on friction and can be controlled to some extent by lubricant additives [6], [7]. To develop an accurate lubrication analysis, the phenomenon of rupture and reformation of the lubricating film is taken into account.

The cavitation phenomenon as well as its principal causes (noise, erosion, etc.) are far from being understood and necessitate further investigations.

In effect, although this phenomenon has been studied by many authors, e.g. for square and circular plates [8] and journal bearing [9], it still remains unknown for the lubrification of the piston skirt.

To contribute to the clarification of the latter problem we have developed a hydrodynamic lubrication model that takes into account the effect of the elasticity of the surfaces separated by the lubricant film and the effect of cavitation.

2. Theoretical modelling

2.1. Basic equations

All the governing equations were given and described by Mazouzi et al. [10]. The equations of motion were derived from the relation based on dynamic equilibrium of all the forces and moments applied to the piston. They can be expressed in matrix form as

$$\begin{bmatrix} m_p\left(1-\frac{b}{L}\right)+m_a\left(1-\frac{a}{L}\right) & m_p\frac{b}{L}+m_a\frac{a}{L} \\ \frac{I_p}{L}+m_p(a-b)\left(1-\frac{b}{L}\right) & m_p(a-b)\frac{b}{L}-\frac{I_p}{L} \end{bmatrix} \begin{bmatrix} \ddot{e}_h \\ \ddot{e}_b \end{bmatrix} = \begin{bmatrix} F+F_s+F_f tan\Phi \\ M+M_s+M_f \end{bmatrix} \quad (1)$$

In these equations, a, b and L are geometric parameters (Fig. 1 and 2) and m_p and m_a are masses of the piston and the wrist-pin respectively. I_p is the rotary inertia of the piston about its center of gravity.

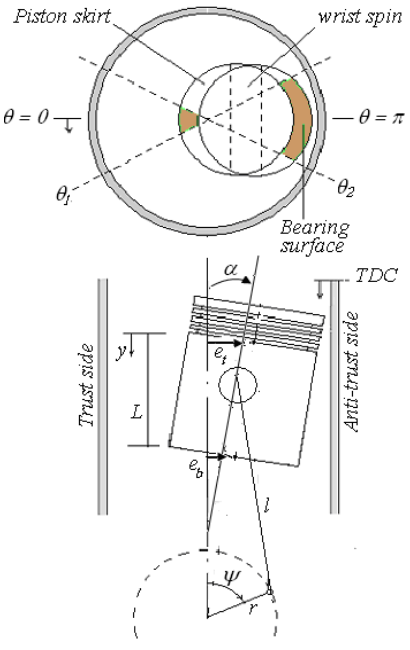

Fig. 1 Piston / cylinder system

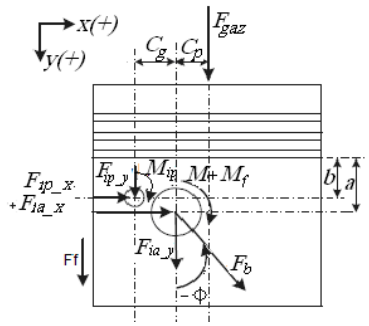

Fig. 2 Forces and moments acting on the piston

The Reynolds equation, which governs the generation of hydrodynamic pressure, is written as

$$\frac{\partial}{\partial y}\left(\frac{h^3}{6\mu}\frac{\partial p_h}{\partial y}\right)+\frac{1}{R^2}\frac{\partial}{\partial \theta}\left(\frac{h^3}{6\mu}\frac{\partial p_h}{\partial \theta}\right)=U\frac{\partial h}{\partial y}+2\frac{\partial h}{\partial t} \quad (2)$$

Eq. (2) must be verified for the active zones (zones under pressure).

For the nonactive zones (zones in cavitation), Eq. (2) reduces to Eq. (3) since the pressure in these areas is constant and is equal to the vapour pressure p_{CAV}.

$$U\frac{\partial \rho h}{\partial y}+2\frac{\partial \rho h}{\partial t}=0 \quad (3)$$

$$r=\frac{\rho h}{\rho_0}$$

where ρ_0 is density of the lubricant, one obtains

$$U\frac{\partial r}{\partial y}+2\frac{\partial r}{\partial t}=0 \quad (4)$$

In order to simultaneously treat Eqs. (2) and (4), they are grouped together while using a universal variable, D [11].

The pressure is established and balance with the load applied is achieved in the active zones.

Conservation of mass flow is respected within inactive zones. Thus we have

$$F\frac{\partial}{\partial y}\left(\frac{h^3}{6\mu}\frac{\partial D}{\partial y}\right)+F\frac{1}{R^2}\frac{\partial}{\partial \theta}\left(\frac{h^3}{6\mu}\frac{\partial D}{\partial \theta}\right)=$$
$$=U\frac{\partial h}{\partial y}+2\frac{\partial h}{\partial t}+(1-F)\left(U\frac{\partial D}{\partial y}+2\frac{\partial D}{\partial t}\right) \quad (5)$$

For the active zones

$$\begin{cases} D=p \\ F=1 \end{cases} \quad (6)$$

Considering the cavitation pressure as the reference pressure, D will be greater than 0 in active zones.

For nonactive zones

$$\begin{cases} D=r-h \\ F=0 \end{cases} \quad (7)$$

As density of the mixture in nonactive zone is always less than ρ_0, D will be less than 0.

For any point of the lubricant film, the compatibility between the sign of D and the inferred state (active or nonactive) of the lubricant film at this point should be verified.

The general boundary conditions for the Reynolds equation are given below

$$\begin{cases} P_h(\theta,y)=0 & y=0, y=L \\ \dfrac{\partial P_h}{\partial \theta}=0 & \theta=0, \theta=\pi \\ P_h(\theta,y)=0 & \theta_1\le\theta\le\theta_2 \end{cases} \quad (8)$$

Thickness of the oil film between the skirt and cylinder wall can be well approximated by

$$h=e_h\cos\theta+(e_b-e_h)\frac{y}{L}\cos\theta+q(y)+h_e \quad (9)$$

where $q(y)$ is nominal geometric thickness of the oil film at y-coordinate for an arbitrary skirt axial profile, and h_e is the thickness due to elastic deformation of the skirt.

Using the finite element method (FEM) a compliance matrix $[C]$ is calculated using the software ACCEL to determine radial displacement of mesh nodes on the elastic skirt surface. The expression of film thickness at a node i is given by the following equation

$$h_e^{\,i}=\sum_{k=1}^{n}C(i,k)F_k \quad (10)$$

where $C(i,k)$ is the elastic compliance matrix representing the displacement at the node i due to a unit force at node k. To obtain a matrix, a unit load is applied successively at each node n of the structure belonging to the wall of the film. The normal displacement at each node of the wall is then calculated.

F_k is the force applied at node k of the lubricant film resulting from pressure field and contact pressure on that node.

The calculation of elastic deformation is given in detail in reference [12].

2.2. Contact pressure

For a typical piston skirt surface, roughness is usually much smaller than waviness, and the wave length is much larger than the wave height. The geometric model of surface waves is shown in Fig. 3. The contact pressure P_c can be resolved starting with the following correlation

$$\delta_i=x_i\left[-0.635ln\left(\frac{x_iL_w}{4\Omega}\right)+1.0556\right] \quad (11)$$

where Ω and L_w are height and length of the wave, respectively. At a certain location, the mean film thickness h becomes smaller than the surface waviness Ω, solid-solid wavy contacts between the piston skirt and the cylinder bore will take place. The local wavy contact deformation can be determined by

$$\delta = \begin{cases} \Omega - h, & \text{if} \quad h < \Omega \quad \left(\dfrac{h}{\Omega} < 1\right) \\ 0, & \text{if} \quad h \geq \Omega \quad \left(\dfrac{h}{\Omega} \geq 1\right) \end{cases} \tag{12}$$

Thus, at any time t, δ is known if h is known, and the quantity x_i can be solved from Eq. (11). The contact pressure P_c is given by

$$P_c = x_i \frac{E'}{L_w}$$

here E' is the Young's elastic modulus. To avoid repeated calculations and minimize the computation time, we use the formula given by Zhu and coworkers in reference [13], relating to an aluminum piston

$$P_c = 5.464 \times 10^{13} \delta^{1.0552} \tag{13}$$

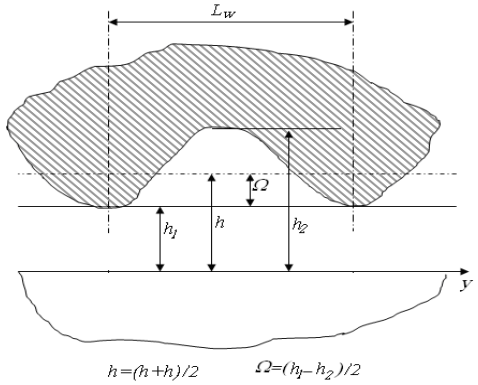

Fig. 3 Waviness: the basic model

2.3. Friction force

The total frictional force on the piston skirt F_f, is given by the sum of two components, hydrodynamic friction F_{fh}, and contact friction F_{fc}

$$F_f = F_{fh} + F_{fc} \tag{14}$$

In Eq. (14), the frictional force due to hydrodynamic lubrication F_{fh}, is given by

$$F_{fh} = 2R \int_0^{\pi} \int_0^{L} \tau \, d\theta dy \tag{15}$$

where

$$\tau = -\frac{\mu U}{h} + \frac{h}{2} \frac{\partial P_h}{\partial y} \tag{16}$$

and the frictional force due to boundary lubrication F_{fc}, is given by

$$F_{fc} = -2C_f \frac{|U|}{U} R \int_0^{\pi} \int_0^{L} P_c \, d\theta dy \tag{17}$$

where τ is the shear stress acting on the piston skirt surface and c_f is the boundary friction coefficient.

On the other hand, the instantaneous power loss is defined by

$$P_u = F_f U \tag{18}$$

where $F_f = F_{fh} + F_{fc}$.

This friction force is useful for assessing where, during the engine cycle, friction is generated, and what parameters contribute to friction. For reporting actual friction losses in an engine, however, another measurement is used. This is the friction mean effective pressure (FMEP) which is the friction work normalized by engine displacement, and is given by

$$FMEF = \frac{\int_{cycle} F_f dy}{V_d} \tag{19}$$

where V_d is the displaced volume of the cylinder (or of the entire engine, if the friction work is also evaluated for the entire engine).

2.4. Analysis of temperature and viscosity

In order to calculate the change in viscosity as a function of temperature, the temperature profile must first be determined. The oil temperature varies slightly between the top of the skirt and the bottom of the skirt, and it varies quite substantially between the top dead centre (TDC) and bottom dead centre (BDC) positions. To determine the profile the Woschni correlation [14] is used

$$T(x) = T_{TDC} - \left(T_{TDC} - T_{BDC}\right)\sqrt{\frac{x}{S}} \tag{20}$$

where $T(x)$ is the liner temperature, presumed to be the same as the lubricant temperature, x is the liner location (measured downward from TDC), T_{TDC} and T_{BDC} are temperatures at TDC and BDC.

The dependence of viscosity on temperature is estimated by using the Vogel equation [15]

$$\mu(T) = \rho a_0 exp\left[\theta_1 / \left(\theta_2 + T\right)\right] \tag{21}$$

where a_0, θ_1 and θ_2 are Vogel correlation parameters.

To study the influence of viscosity on the contact parameters, we use oils with different viscosity grades. Table 1 lists the parameters used in the Vogel equation.

Table 1
Vogel parameters used for calculating viscosity [15]

Oil	ρ, kg/m^3	a_0, cst	θ_1, ℃	θ_2, ℃
SAE-20	832	0.0580	1028	108.0
SAE-30	839	0.0274	1361	123.3
SAE-50	852	0.0223	1518	122.6

3. Numerical procedure

The numerical procedure is summarized as follows.

1. Initialization of the oil film thickness h, eccentricities e_t, e_b and pressures P_h and P_c.
2. Calculation of the average temperature and corre-

sponding oil film viscosity.

3. Calculation of the elastic deformation due to total pressure forces ($P_h + P_c$) using Eq. (10). Calculation of the total film thickness using Eq. (9).

4. Computation of D (modified Reynolds equation)
   Update of the partition:
   - when $D<0$ the node becomes non-active;
   - when $D\geq 0$ the node becomes active.

5. Numerical resolution of equilibrium equations and the Reynolds equation by the Newton-Raphson method after discretization by finite differences. Thus the hydrodynamic pressure distribution is calculated, and the new contact pressure is calculated using Eq. (13).

6. Determination of all hydrodynamic and contact forces and moments acting on the piston.

7. Repeat steps 2, 3, 4, 5 and 6 until solution convergence is obtained, that is until the following criteria are satisfied.

$$\left|\frac{P_{h,ij}^{\ k}-P_{h,ij}^{\ k-1}}{P_{h,ij}^{\ k}}\right| \langle 10^{-4} \qquad \left|\frac{e_h^{\ k}-e_h^{\ k-1}}{e_h^{\ k}}\right| \langle 10^{-3}$$

$$\left|\frac{e_b^{\ k}-e_b^{\ k-1}}{e_b^{\ k}}\right| \langle 10^{-3}$$

With a time step that corresponds to 5 degrees of crankshaft angle, convergence is reached after 4 to 5 motor cycles.

4. Results and discussion

The numerical simulation was performed on a small four-stroke engine, the input data are listed in Table 2.

Table 2

Geometry and simulation data

Parameters	Values
Diameter of piston, m	83.10^{-3}
Radius of crankshaft, m	$41.8.10^{-3}$
Length of connecting rod, m	133.10^{-3}
Piston skirt length, m	$33.8.10^{-3}$
Piston skirt angle, degrees	37.5
Radial clearance, m	$20.50.10^{-6}$
Cp, m	1.10^{-3}
Cg, m	2.10^{-3}
A, m	$12.5.10^{-3}$
B, m	$1.5.10^{-3}$
Mass of wrist-pin, Kg	0.09
Mass of piston, Kg	0.295
Wave height, m	$3.50.10^{-6}$
Engine speed, tr.min-1	1000
Coefficient of friction for solid-to- solid contacts	0.150

Fig. 4 shows the variation of viscosity during the cycle. On average, the viscosity varies by a factor of 2 between the top dead center and bottom dead center. Note the approximately sinusoidal nature of this variation as the piston moves up and down on the liner, this variation is related to the temperature distribution (Fig. 5). The pressure is maximal near TDC just after firing. The TDC position corresponds to the crankshaft angles 0, 360 and 720° representing the trough of the curve in Fig. 4, when the viscosity is low and lateral pressure is high. This area is most vulnerable to boundary friction and its concomitant wear.

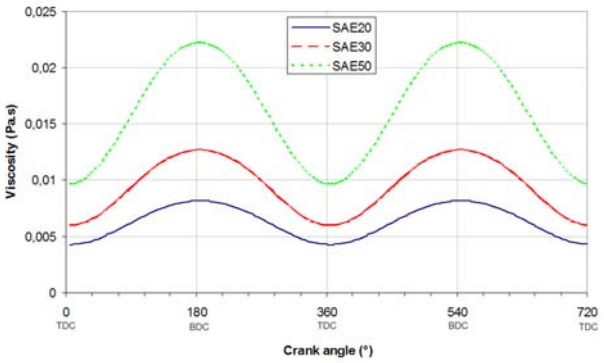

Fig. 4 Viscosity versus crank angle during the cycle

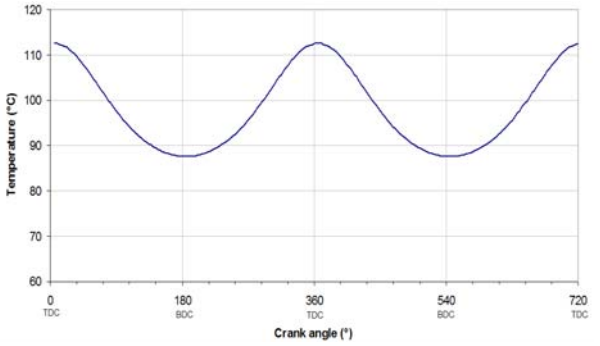

Fig. 5 Temperature distribution in the middle of the skirt in relation to the crankshaft angle

Figs. 6 and 7 show the effect of viscosity on the minimum oil film thickness (MOFT) and the maximum hydrodynamic pressure. The maximum values of MOFT increase with increasing viscosity.

With SAE-50 oil, the lubricant film is thicker and there is no solid-solid contact, especially during the intake and compression stroke. During the expansion stroke, the maximum hydrodynamic pressure and the viscosity of the oil film are inversely proportional. In fact, this pressure is about 31, 17 and 12 MPa for SAE 20, SAE-30 and SAE-50 oils, respectively.

Figs. 8 and 9 show the variation of total friction force and power loss for three different oils as a function of the crankshaft angle. Although high viscosity oil produces greater friction work by increasing shear stresses, the greater shear stresses enable it to support a greater load (at a given sliding speed).

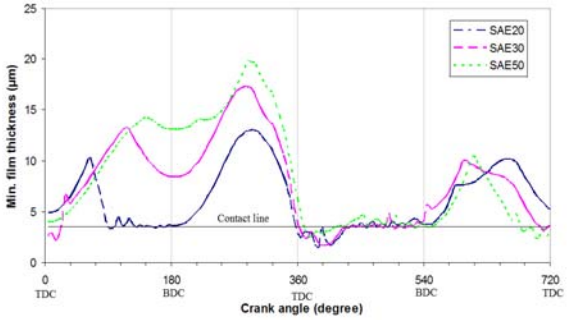

Fig. 6 Effect of oil viscosity on minimum film thickness at 1000 r/min

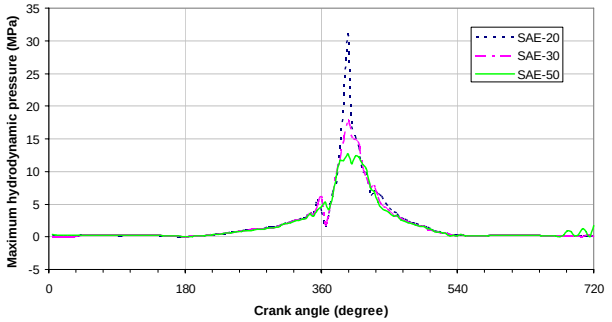

Fig. 7 Effect of oil viscosity on maximum hydrodynamic pressure at 1000 r/min

The ability of viscous oils to sustain loads is essential for piston support, since this property helps to avoid direct contact between the components. The friction power loss is greater with a high viscosity grade. The reduction of viscosity is a potential method for reducing friction. However, if the viscosity is reduced below the level required for hydrodynamic support, the piston surface will contact the liner surface and incur boundary contact friction.

Between angles 360 and 400 degrees, Figs. 8 and 9 show a particular behaviour. This represents the starting of the explosion power stroke in which the gases force is very high and the piston tilt reaches its maximum value. The minimum film thickness becomes smaller than the wave height (Fig. 6). At this moment the contact force prevails. This contrasts with the other phases in which the hydrodynamic force is the dominant one.

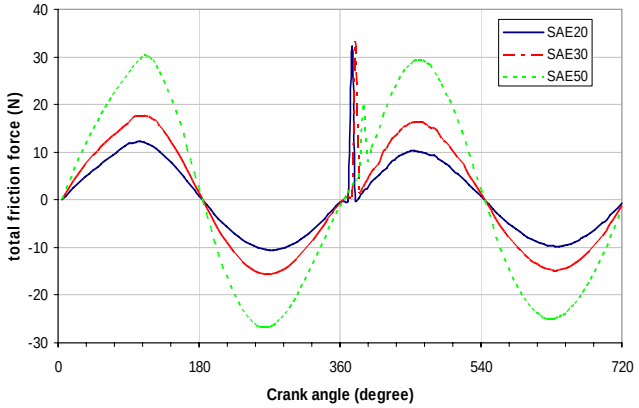

Fig. 8 Friction force during the cycle for different lubricants

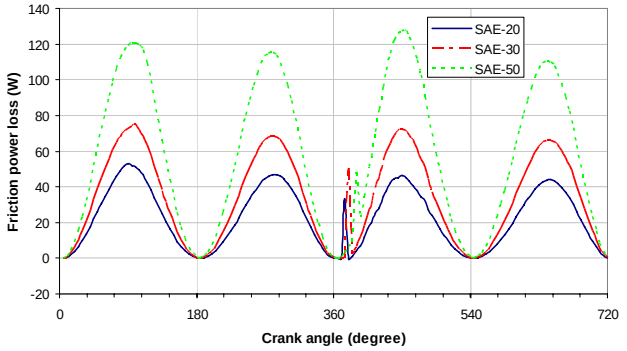

Fig. 9 Friction power loss during the cycle for different lubricants

The Stribeck curve Fig. 10 indicates how the effective coefficient of friction depends on the dimensionless parameter $\mu U/w$, where μ is the viscosity, U is sliding speed and w is loading force per unit area. If the viscosity increases and everything else remains constant, the lubrication regime shifts towards the right (i.e., towards the hydrodynamic part) of the curve.

Generally, the sliding speed U is fixed by engine speed and geometry, and loading force per unit area w is fixed by the cylinder pressure and connecting-rod geometry. Consequently, viscosity is the only significant parameter in the Stribeck curve that can be modified.

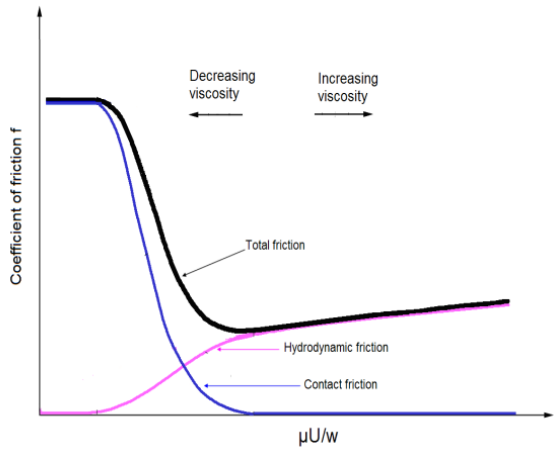

Fig. 10 Stribeck curve, showing how changing viscosity affects friction

Table 3 summarizes the results relating to the minimum film thickness, hydrodynamic pressure and friction power loss for various lubricants.

Table 3
Sensitivity of tribological parameters to lubricant viscosity grade at 1000 rpm

Lubricant	Minimum oil film thickness, μm	Maximum hydrodynamic pressure, MPa	Average friction power loss, W
SAE-20	1.45	24.01	22.5
SAE-30	1.71	16.06	33.8
SAE-50	1.79	12.35	57.6

Table 3 shows clearly that reductions in piston skirt friction can be achieved by using a lubricant of lower viscosity. However, this is at the expense of lower MOFT. In Table 3 we can see that moving from an SAE-50 lubricant to an SAE-20 lubricant will lead to a 20% decrease in minimum oil film thickness, and will also yield a decrease in piston skirt friction of approximately 40%, against a 50% increase in maximum hydrodynamic pressure.

The benefits of moving to lower viscosity lubricants to obtain better fuel efficiency through lower engine friction have been well documented [16].

Reducing the piston skirt/liner boundary friction coefficient can provide a great advantage to the functioning of the mechanism. This reduction is possible in practice, for example by modifying lubricant additives, or by selecting the appropriate materials for the piston and liner. Decreasing the boundary friction coefficient C_f, reduces piston skirt / liner friction both directly, by reducing the friction due to asperity contact, and indirectly, by allowing lubricant viscosity to be reduced and thus also reducing hydrodynamic friction. This is illustrated in Fig. 11, which shows the dependence of the FMEP skirt/liner on the boundary friction coefficient for different lubricant viscosities.

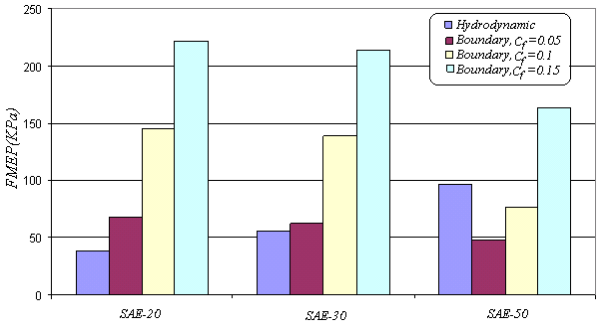

Fig. 11 Effect of the boundary friction coefficient on friction

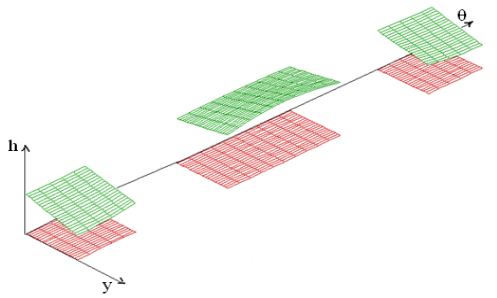

a

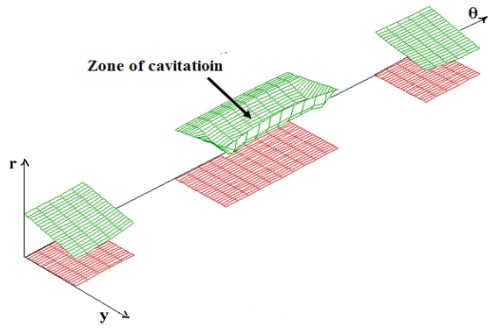

b

Fig. 12 Fields of thickness *h* (a), and replenishment (b) at 345° crank angle

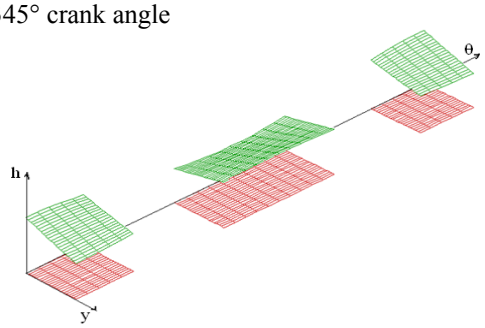

a

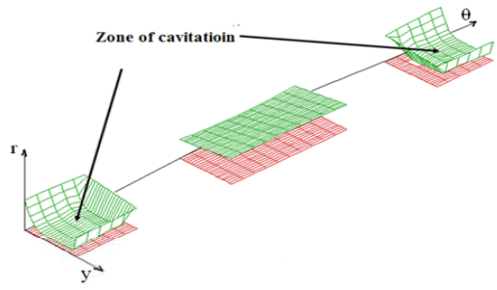

b

Fig. 13 Fields of thickness *h* (a), and replenishment (b) at 560° crank angle

Figs. 12 and 13 shows the fields of thickness *h* and replenishment *r* when the phenomenon of cavitation is taken into account for two crankshaft angles. By comparison between *h* and *r*, we can observe the nonactive zone on the anti-thrust side at 345° crank angle, on the other hand this zone is located on the thrust side at 560° crank angle.

To assess the effect of viscosity on cavitation, we have represented the field of replenishment for two different oils Fig. 14. With SAE-20 oil, the amplitude of the nonactive zone is larger with a smaller replenishment compared to an SAE-30 oil. The cavitation decreases with increasing viscosity.

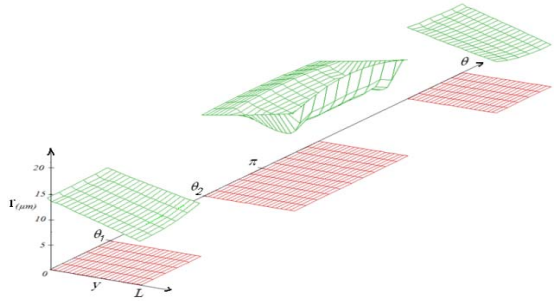

a

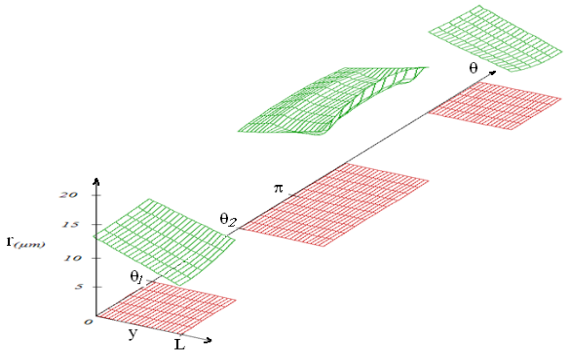

b

Fig. 14 Effect of oil viscosity on cavitation, replenishment for SAE-20 oil (a), and SAE-30 (b)

5. Conclusion

In this article a piston skirt lubrication model is developed. The results of tribological characteristics such as the movement of the piston, the minimum film thickness, the frictional force and friction power loss were studied in relation to the viscosity lubricant. Oil viscosity directly affects friction in the hydrodynamic regime. Indeed, the hydrodynamic friction increases with viscosity. The viscosity also indirectly affects the contact friction by determining the oil film thickness. The reduction in viscosity can reduce the hydrodynamic friction, but also leads to a reduction in the oil film thickness. This makes the contact with asperities more likely. The best design involves obtaining a system that operates principally in a hydrodynamic lubrication regime using low viscosity oil. Reducing the boundary coefficient friction value allows the use of a low viscosity oil and leads to a balance between hydrodynamic lubrication and boundary lubrication. Using the modified Reynolds equation allows us to consider the phenomenon of rupture and reformation of the film and identify the zones of cavitation in different places depending on the crank angle. With high viscosity, the phenomenon of cavitation is reduced significantly.

References

1. **Zhu, D., and Cheng, H.S.** A numerical analysis for piston skirt in mixed lubrication - Part II: Deformation considerations. -ASME Journal of Tribology, 1993, v.115, p.125-133.
2. **Liu, K., Xie, Y.B.**, **Gui, C.L.** A comprehensive study of the friction and dynamic motion of the piston assembly. -Proc. Instn. Mech. Engrs., Part J, 1998, v.212, p.221-226,
3. **Balakrishnan, S., Rahnejat, H.** Isothermal transient analysis of piston skirt-to- cylinder wall contacts under combined axial, lateral and tilting motion.-J. Phys. D: Appl. Phys. 2005, 38, p.787-799.
4. **Richardson, D.E., Borman, G.L.** Theoretical and experimental investigations of oil films for application to piston ring lubrication.-SAE Technical Paper, No.SAE-922341, 1992, p.105-120.
5. **Taylor, R.I.** Engine friction: the influence of lubricant rheology. -Proc. Instn. Mech. Engrs., 1997, v.211, part J, p.235-246.
6. **Dagilis, V., Vaitkus, L.** Experimental investigations and analysis of compressor's friction losses. -Mechanika. -Kaunas: Technologija, 2009, Nr.5(79), p.28-35.
7. **Himanshu, C. Patel, Deheri, G. M.** Characteristics of lubrication at nano scale on the performance of transversely rough slider bearing. -Mechanika. -Kaunas: Technologija, 2009, Nr.6(80), p.64-71.
8. **Boedo, S., Booker, J.F.** Cavitation in normal separation of square and circular plates. -ASME Journal of Tribologie, 1995, v.117, p.403-410.
9. **Optasanu, V., Bonneau, D.** Finite element mass-conserving cavitation algorithme in pure squeeze motion. Validation - application to a connecting - rod small end bearing. -ASME Journal of Tribologie, 1999, v.122, p.162-169.
10. **Mazouzi, R., Maspeyrot, P., Kellaci, A., Rahal, D.D.** Effet des paramètres de conception du piston sur le frottement jupe-chemise, Revue Mécanique et Industrie, 2009, v.10, p.91-101.
11. **Hajjam, M., Bonneau, D.** A transient finite element cavitation algorithm with application to radial lip seals. -Journal of Tribology International, 2007, v.40, p.1258-1269.
12. **Bonneau, D., Hajjam, M.** Modélisation de la rupture et de la reformation des films lubrifiants dans les contacts elastohydrodynamiques.-Rev. Euro. Eléments Finis, 2001, v.10 10, p.679-704.
13. **Zhu, D., Cheng, H.S.** A numerical analysis for piston skirt in mixed lubrication - Part I: Basic modelling. -ASME Journal of Tribology, 1992, v.114, p.553-562.
14. **Woschni, G., Zeilinger, K.** Vorausberechnung des Kolbenringverhaltens. -FFV Workshop, Tribosystem Kolben-Kolbenring-Zylindgerlaufflache, 10, okt., 1989, VDMA-Haus Frankfurt.
15. **Cameron, A.** Basic Lubrication Theory. Third Edition. -Ellis Horwood Ltd., 1983.
16. **Taylor, R.I., Coy, R.C.** Improved fuel efficiency by lubricant design: A review. -Proc. Instn. Mech. Engrs., 2000, v.214, part J, p.1-15.

A. Kellaci, R. Mazouzi, B. Khelidj, A. Bounif

TEPALO REOLOGIJOS POVEIKIS VIDAUS DEGIMO VARIKLIO STŪMOKLIO IR CILINDRO KONTAKTUI

R e z i u m ė

Nagrinėta įvairių monogradinių tepalų klampumo įtaka hidrodinaminei bei ribinei vidaus degimo variklio trinčiai stūmoklio paviršiuje. Vidutinė temperatūra nustatyta pagal įvorės temperatūrą, naudojant Woschni koreliaciją. Tepalo plėvelės klampumas nustatytas pagal vidutinę jos temperatūrą. Šis modelis įvertina tepalo plėvelės suirimo ir atsinaujinimo procesą. Straipsnyje taip pat nagrinėta tepalo klampumo įtaka kavitacijai.

A. Kellaci, R. Mazouzi, B. Khelidj, A. Bounif

THE EFFECT OF LUBRICANT RHEOLOGY ON PISTON SKIRT/CYLINDER CONTACT FOR AN INTERNAL COMBUSTION ENGINE

S u m m a r y

The sensitivity of internal combustion engine friction to lubricant viscosity has been studied. The effect of oil viscosity on the hydrodynamic and boundary friction of the piston skirt has been discussed with various monograd lubricants. The average temperature is determined from the temperature of the liner using the Woschni correlation. The oil film viscosity is then estimated using the mean temperature of the oil film. This model takes into account the phenomenon of rupture and reformation of the oil film. The effect of viscosity on cavitation is also studied.

А. Келлаци, Р. Мазоузи, Б. Кхелидй, А. Боуниф

ВЛИЯНИЕ РЕОЛОГИИ СМАЗКИ НА КОНТАКТ ЮБКИ ПОРШНЯ/ЦИЛИНДРА В ДВИГАТЕЛЕ ВНУТРЕННЕГО СГОРАНИЯ

Р е з ю м е

Исследовано влияние вязкости смазки на трение в двигателе внутреннего сгорания. Обсуждено влияние вязкости смазки на гидродинамическое и граничное трение на юбке поршня при использовании различных моноградных смазок. Средняя температура определена по температуре юбки используя Восхни (Woschni) корреляцию. Вязкость смазочной пленки рассчитана по средней ее температуре. Приведенная модель оценивает процесс разрушения и восстановления смазочной пленки. В статье также рассмотрено влияние вязкости смазки на кавитацию.

Received October 29, 2009
Accepted January 15, 2010

DOI: 10.5755/j02.mech.9765